



## A planar capacitive sensor for 2D long-range displacement measurement\*

Jian-ping YU<sup>1</sup>, Wen WANG<sup>†‡2</sup>, Ke-qing LU<sup>2</sup>, De-qing MEI<sup>1</sup>, Zi-chen CHEN<sup>1</sup>

<sup>1</sup>Department of Mechanical Engineering, Zhejiang University, Hangzhou 310027, China)

<sup>2</sup>School of Mechanical Engineering, Hangzhou Dianzi University, Hangzhou 310018, China)

<sup>†</sup>E-mail: wangwn@hdu.edu.cn

Received Oct. 9, 2012; Revision accepted Jan. 9, 2013; Crosschecked Mar. 11, 2013

**Abstract:** A planar capacitive sensor (PCS) capable of 2D large-scale measurement is presented in this paper. Displacement interpretation depends on independently measuring the periodic variation in capacitance caused by the change in the overlapping area of sensing electrodes on a moving plate and a fixed plate. By accumulating the number of quarters in each direction and the specific position in the final quarter, the large-scale measurement is fulfilled. Displacements in *X*- and *Y*-direction can be measured independently and simultaneously. Simulation shows that a shorter gap distance and a longer electrode guarantee better sensitivity. Experiments based on a PCS test bench demonstrate that the PCS has a sensitivity of 0.198 mV/μm and a resolution of 0.308 μm. An electric fringe effect and other possible measurement errors on displacement interpretation accuracy are discussed. The study confirms the high potential of PCSs as innovative 2D long-range displacement sensors.

**Key words:** Planar capacitive sensor (PCS), Displacement measurement, 2D large-scale measurement

**doi:**10.1631/jzus.C12MNT03

**Document code:** A

**CLC number:** TH711; TB92

### 1 Introduction

Precision measurement in nanometer accuracy is of profound importance for the development of nanotechnology, particularly for biomedical devices, intelligent instruments, portable electronic devices, and precision positioners. Currently, several kinds of precise displacement measuring methods and sensors have been developed into applications (Tolles, 1996; Baxter, 1997; Chang and Lee, 2010), including capacitive sensors, gratings, and laser interferometers. A capacitive sensor is limited to a short-stroke of several millimeters. A grating has a large-scale measuring range but needs more mounting space, especially for

multi-dimensional measurement. A laser interferometer offers both high accuracy and long range, but its work performance is easily affected by the environment.

Limited by their short-stroke, capacitive sensors were usually considered most suitable for circumstances that require non-contact measurements with micro-scale range and nano-scale resolution. Recently, to accomplish nano-scale resolution and large-scale measurement, planar capacitive sensors (PCSs) have been gaining more acceptance as an alternative means of precise displacement measurement. The last decades have seen a large increase in research on PCSs. Linear PCSs are mostly of encoder-like prototypes and are capable of achieving high sensitivity and a large range of motion. However, when linear PCSs were implemented for multi-dimensional measurement, Abbe and cumulative errors would often decrease the measurement accuracy (Meyer, 1996; Pedrocchi *et al.*, 2000; Kim and Moon, 2006; Kuijpers *et al.*, 2006). To avoid such errors, specific designs of

<sup>‡</sup> Corresponding author

\* Project supported by the National Natural Science Foundation of China (No. 51275465), the National Basic Research Program (973) of China (No. 2011CB013300), and the Scientific Research Foundation for the Returned Overseas Chinese Scholars, Ministry of Education, China (No. [2011]1568)

© Zhejiang University and Springer-Verlag Berlin Heidelberg 2013

PCSs have been presented and the measurement accuracy has been improved. However, some of the designs are still limited to a short range of motions (Kolb et al., 1998; Picotto et al., 2009; Huang et al., 2010). Some researchers then applied an incremental layout of electrodes on PCSs. Nano-order resolution and large-scale measurement were both achieved (Bonse et al., 1994; Furuichi and Fearing, 1996; Wang et al., 2008).

In this paper, a novel PCS is proposed for use in precise positioning systems, which is capable of realizing 2D long-range displacement measurement independently and simultaneously. Simulation analysis in terms of measurement sensitivity was carried out, and a PCS test bench was constructed. The results of experiments led to the conclusion that PCSs have high potential as innovative 2D long-range displacement sensors.

## 2 Principle of a planar capacitive sensor

A PCS consists of a moving plate (MP) and a fixed plate (FP) (Fig. 1) (Wang et al., 2008). On the MP, square capacitive electrodes of the same size are periodically positioned and electrically connected to a driving voltage  $V_{input}$ , where  $P=2l$  is the interval length (for both the  $X$  and  $Y$  directions),  $l$  is the length of the electrodes, and  $d$  represents the gap distance. The FP is similarly designed, but to realize 2D displacement measurement, electrodes on the FP have a specific arrangement.

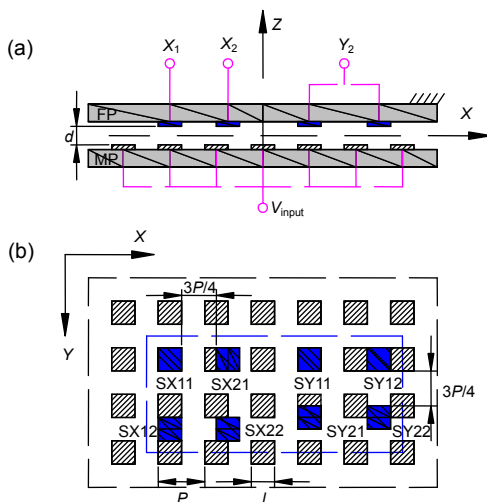


Fig. 1 Schematic views of a 2D planar capacitive displacement sensor: (a) front view; (b) cross view

The principle of displacement measurement is based on measuring the periodic change of capacitance between a sensor array on the MP and the FP. When the MP moves, the overlapping area of the electrodes changes periodically, which is proportional to the capacitance change. To detect  $X$  and  $Y$  displacements simultaneously and incrementally, the sensor array on the FP is divided into four groups, each including two electrodes, i.e., group SX1 (including two electrodes, SX11 and SX12), SX2 (SX21, SX22), SY1 (SY11, SY12), and SY2 (SY21, SY22). Signals from the electrodes are defined as  $X_1$ ,  $X_2$ ,  $Y_1$ , and  $Y_2$ . Since SX1 and SY1 are  $90^\circ$  out-of-phase to SX2 and SY2, respectively,  $(X_1, X_2)$  and  $(Y_1, Y_2)$  represent two sets of quadrature signals available for signal interpolation.

First, suppose that the MP and FP are in the position shown in Fig. 1. When the MP moves in the  $X$  direction, the overlapping area of (SX11+SX12) changes as a triangular waveform, and the relevant change in capacitance ( $C_{SX11}+C_{SX12}$ ) is proportional to the displacement in the  $X$  direction. For the capacitance ( $C_{SX11}+C_{SX12}$ ):

$$C_{SX11}+C_{SX12}=C_{SX11}. \tag{1}$$

Since SY11 and SY12 are differentially positioned, when the MP moves in the  $X$  direction, the overlapping area of (SY11+SY12) keeps constant, so the capacitance ( $C_{SY11}+C_{SY12}$ ) does not change. Thus,

$$C_{SY11}+C_{SY12}=1 \text{ (normalized)}. \tag{2}$$

From Eqs. (1) and (2), the  $X$  direction measurement can be calculated by the sum of  $C_{SX11}$  and  $C_{SX12}$ , while the sum of  $C_{SY11}$  and  $C_{SY12}$  can be neglected because of its constant value.

Similarly, when the MP moves in the  $Y$  direction, the overlapping area of (SY11+SY12) changes periodically, and as a result, the relevant change in capacitance ( $C_{SY11}+C_{SY12}$ ) is proportional to the displacement in the  $Y$  direction. In this case, the overlapping area of (SX11+SX12) is kept constant and the relevant capacitance does not change.

Hence, the displacements in the  $X$  and  $Y$  directions depend on the independent periodic changes in capacitance of (SX11+SX12) and (SY11+SY12).

If PCS capacitance can be calculated simply as  $\epsilon_0 \epsilon_r l^2/d$ , where  $\epsilon_0$  is the permittivity in a vacuum and  $\epsilon_r$  is the relative permittivity, then the normalized waveforms of  $C_{SX1}$ ,  $C_{SX2}$ ,  $C_{SY1}$ , and  $C_{SY2}$  are in triangular dependence (Fig. 2) (Baxter, 1997; Wang et al., 2008).

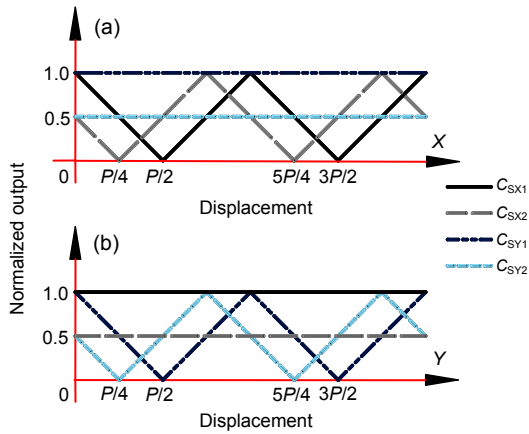


Fig. 2 Normalized waveforms of  $C_{SX1}$ ,  $C_{SX2}$ ,  $C_{SY1}$ , and  $C_{SY2}$ : (a) X direction; (b) Y direction

### 3 Simulation analysis of sensor performance

Sensitivity is the main limitation to improving sensor performance, and depends largely on the structural layout. Thus, here we consider different kinds of structural layouts in a simulation analysis.

When the electrode length  $l$  is more than 10 times longer than the gap distance  $d$ , i.e.,  $l \geq 10d$ , the fringe effect of the PCS can be ignored, and the waveform of PCS can be considered in the triangular model (Baxter, 1997). However, usually the electrode length can be guaranteed to be only five times the gap distance or less, i.e.,  $l \leq 5d$ . So, the fringe effect cannot be ignored and studies have been made to derive a precise capacitance calculation. In this section, the capacitance of a single electrode is derived from Maxwell's equations (Benedek and Silvester, 1972; Pedrocchi et al., 2000):

$$C = \frac{Q}{V_{input}} = -\epsilon_0 \epsilon_r l \left( \frac{l}{2d} - \sum_{n=odd} \frac{4}{k_n l \sinh(k_n d)} \cos(k_n x) \right), \quad (3)$$

where  $Q$  is the quantity of electric charge,  $k_n = n\pi/l$  ( $n=1, 3, 5, \dots$ ),  $x$  is the displacement in the X direction,

and  $V_{input}$  is the voltage applied to the capacitive electrodes.

Then, PCS sensitivity per unit sensor area can be derived as

$$S_{PCS} = NS = N \frac{\partial(\Delta C)}{\partial x} = -\epsilon_0 \epsilon_r N \sum_{n=odd} \frac{4}{l \sinh(k_n d)} \sin(k_n x), \quad (4)$$

which shows that there are three main factors that determine the sensitivity of a PCS: the electrode number  $N$ , the electrode length  $l$ , and the gap distance  $d$ .

The model chosen for simulation was a 2D model (Fig. 1).

1. Analysis of electrode number  $N$ : From Eq. (4), the PCS sensitivity is proportional to the electrode number  $N$ . However, when  $N$  becomes very large, the PCS would become bulky, which should be avoided.

2. Analysis of gap distance  $d$ : Based on Eq. (3), Fig. 3 presents the periodic changes in capacitance per unit sensor area between the MP and the FP with a gap distance ranging from 0.2 to 2.0 mm (i.e.,  $d=0.2, 0.5, \text{ or } 2.0$  mm) when the electrode length is kept constant at 5 mm.

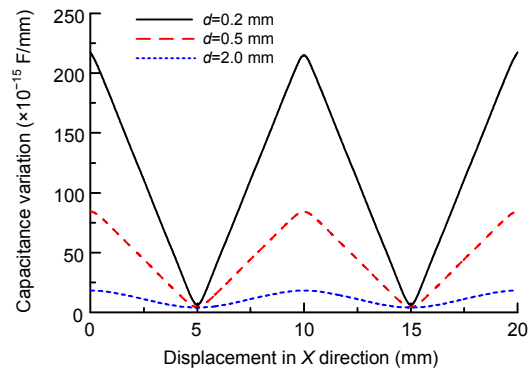


Fig. 3 Periodic variation in capacitance of SX1 per unit sensor area with different gap distances (electrode length  $l=5$  mm)

Table 1 lists the simulation results based on Eq. (4). As the gap distance enlarges, the PCS sensitivity declines sharply. However, a smaller gap distance makes manufacture and assembly more difficult. Surface roughness and tilting would also seriously affect measurement accuracy. Thus, finding a balance between the electrode length  $l$  and the gap distance  $d$  is of paramount importance.

**Table 1** PCS sensitivity corresponding to gap distance \*

Gap distance, $d$ (mm)	$d/l$	Sensitivity per unit sensor area (fF/mm <sup>2</sup> )	Sensitivity ratio
0.2	1/25	39.870	14.650
0.5	1/10	15.256	5.606
2.0	1/2.5	2.721	1.000

\* Electrode length  $l=5$  mm

3. Analysis of electrode length  $l$ : Fig. 4 shows the simulated capacitive variation per unit sensor area between the MP and the FP calculated based on Eq. (3) when electrode length varies from 1 to 5 mm (i.e.,  $l=1, 2,$  or  $5$  mm), and the gap distance  $d$  is kept constant at 0.5 mm.

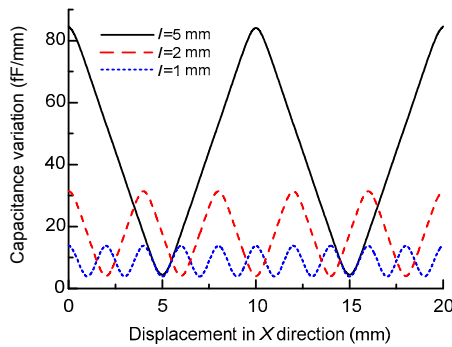


**Fig. 4** Periodic variation in capacitance of SX1 per unit sensor area with different electrode lengths (gap distance  $d=0.5$  mm)

Table 2 lists the simulation results. A PCS with a 5 mm-long electrode has a sensitivity per unit sensor area as high as 15.256 fF/mm<sup>2</sup>, which is about 1.617 times that of a PCS with a 1 mm-long electrode. The main reason for this is that the field fringe effect has a more severe impact on a PCS with a shorter electrode. This analysis indicates that increasing the electrode length provides a feasible way of increasing the PCS sensitivity. However, a larger electrode means a larger PCS, and the sensor system could easily become bulky.

**Table 2** Planar capacitive sensor (PCS) sensitivity corresponding to electrode length \*

Electrode length, $l$ (mm)	$d/l$	Sensitivity per unit sensor area (fF/mm <sup>2</sup> )	Sensitivity ratio
1	1/2	9.437	1.000
2	1/4	13.094	1.388
5	1/10	15.256	1.617

\* Gap distance  $d=0.5$  mm

## 4 Experimental results

From the analysis in Section 3, we conclude that a smaller gap distance and a longer electrode guarantee better sensitivity. Thus, in our experiments, the electrode length and gap distance of the PCS were defined as 5 and 0.5 mm, respectively.

Fig. 5 depicts the test bench of the PCS system. The MP was mounted on a precision linear motion system, and the FP was fixed with a clamping set.

A sinusoidal voltage  $V_{input}$  with a frequency of 10 kHz generated by a GWINSTEK<sup>®</sup> GFG-8016G model signal generator was applied to the electrodes on the MP. The voltage amplitude was limited to the rated voltage of the amplifier, at under 2.5 V.

Since the  $X$  and  $Y$  displacement measurements are similarly designed, in the experiment, the estimation of PCS performance was carried out only in the  $X$  direction. Fig. 6 gives the output voltages from electrode groups SX1 and SX2, when the FP had 20 mm movement in the  $X$  direction.

The data acquisition system used in the experiment was an NI<sup>®</sup> USB-6259BNC 16-bit data acquisition (DAQ) card with an input range of  $\pm 2$  V. From the results shown in Fig. 6, the actual PCS sensitivity can be defined as

$$S = \frac{U_{avg}}{P/2} = \frac{989.77 \text{ mV}}{5000 \mu\text{m}} \approx 0.198 \text{ mV}/\mu\text{m}, \quad (5)$$

where  $U_{avg}$  represents the average amplitude of the output voltage  $X_1$  under different periods.

Then, the PCS resolution  $R$  can be calculated as

$$R = \frac{4 \text{ V} \times P/2}{(2^{16} - 1)U_{avg}} = 0.308 \mu\text{m}. \quad (6)$$

The nominal demodulated PCS outputs are assumed to be in perfect triangular waveform models. However, output signals from the PCS have different kinds of waveform errors, and displacement measurement accuracy is severely affected because of the following problems:

1. Displacement is in reality a distorted (rounded) triangular dependence. The fringe effect is the main reason for waveform distortion. By loading a triangular linear fitting on output signal  $X_1$ , the maximum waveform deformation errors of each period can be

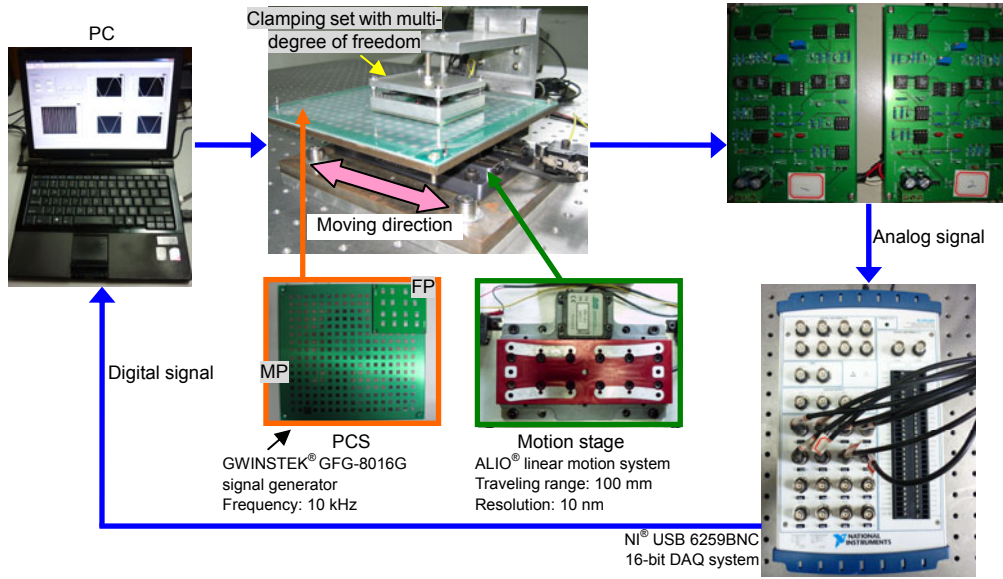


Fig. 5 Test bench of the planar capacitive sensor (PCS) system

shown to range from 40 to 50 mV (Fig. 7). Derived from the demodulated output voltage of  $X_1$  at 20 mm displacement, the maximum error is 46.91 mV. The equivalent displacement error is calculated as

$$x_{\text{error}}^1 = \frac{\sigma_{\text{max}}}{U_{\text{avg}}} \times 5 \text{ mm} = \frac{46.91 \text{ mV}}{989.77 \text{ mV}} \times 5 \text{ mm} \approx 0.237 \text{ mm}. \quad (7)$$

2. PCS un-parallelism, caused mainly by surface roughness and installation errors, would result in waveform amplitude errors. Derived from the demodulated output voltage of  $X_1$  in Fig. 6, the peak-peak voltage error from the first period to the adjacent period is 27.82 mV, and the equivalent displacement interpretation error is

$$x_{\text{error}}^2 = \frac{U_{\text{pk-pk}}^{\text{error}}}{U_{\text{avg}}} \times 5 \text{ mm} = \frac{27.82 \text{ mV}}{989.77 \text{ mV}} \times 5 \text{ mm} \approx 0.141 \text{ mm}. \quad (8)$$

From the experimental results, the following steps should be taken to improve the PCS performance: (1) A PCS capacitance model should be reconstructed in consideration of an electric field fringe effect. Eq. (3) presents a preliminary model, but a more simplified and refined model is required. (2) Installation accuracy and system stability needs to be guaranteed.

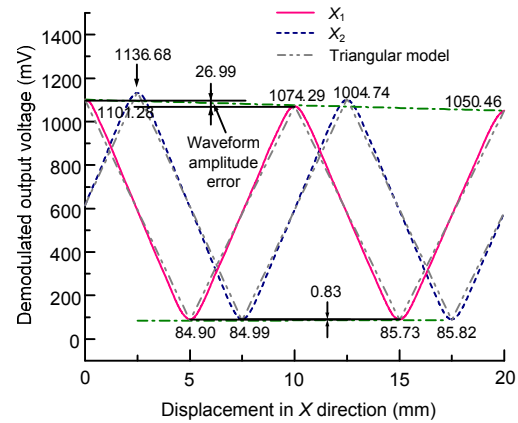


Fig. 6 Demodulated output voltages of SX1 and SX2 during 20 mm displacement in the X direction

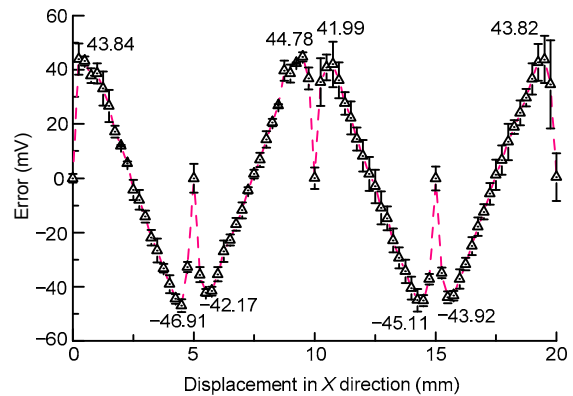


Fig. 7 Waveform deformation errors of  $X_1$  in a triangular waveform model during 20 mm displacement in the X direction

## 5 Conclusions

In this paper, a novel design of a PCS for 2D large-scale measurement is presented. Structural analysis in terms of PCS sensitivity was carried out. A smaller gap distance and a longer electrode mean better sensitivity. As a result, a gap distance of 0.5 mm and an electrode length of 5 mm were applied in the actual PCS model.

Experiments based on a PCS prototype were performed. From the results, a sensitivity of 0.198 mV/ $\mu\text{m}$  was attained. PCS resolution was limited to 0.308  $\mu\text{m}$  by the DAQ system. PCS measurement accuracy was severely affected by two problems: firstly, a fringe effect caused a 237- $\mu\text{m}$  position deviation; secondly, PCS un-parallelism, caused mainly by surface roughness and installation error, induced a 141- $\mu\text{m}$  position error.

Future research should focus on improving PCS fabrication accuracy and reducing installation errors. System-on-a-chip (SoC) manufacturing technology should also be adopted to construct a capacitance DAQ system to lower the interference from parasitic capacitance and electric cables.

## References

- Baxter, L.K., 1997. *Capacitive Sensors: Design and Applications*. IEEE Press, Piscataway, NJ.
- Benedek, P., Silvester, P., 1972. Capacitance of parallel rectangular plates separated by a dielectric sheet. *IEEE Trans. Microw. Theory Tech.*, **20**(8):504-510. [doi:10.1109/TMTT.1972.1127797]
- Bonse, M.H.W., Zhu, F., Spronck, J.W., 1994. A new two-dimensional capacitive position transducer. *Sens. Actuat. A*, **41**(1-3):29-32. [doi:10.1016/0924-4247(94)80082-0]
- Chang, S., Lee, J., 2010. Design of a long range nano-scale resolution mechanism. *J. Zhejiang Univ-Sci. A (Appl. Phys. & Eng.)*, **11**(4):250-254. [doi:10.1631/jzus.A1000029]
- Furuichi, H., Fearing, R.S., 1996. A Planar Capacitive Micro Positioning Sensor. Proc. 7th Int. Symp. on Micro Machine and Human Science, p.85-90. [doi:10.1109/MHS.1996.563406]
- Huang, X.H., Lee, J.I., Ramakrishnan, N., Bedillion, M., Chu, P., 2010. Nano-positioning of an electromagnetic scanner with a MEMS capacitive sensor. *Mechatronics*, **20**(1):27-34. [doi:10.1016/j.mechatronics.2009.06.005]
- Kim, M., Moon, W., 2006. A new linear encoder-like capacitive displacement sensor. *Measurement*, **39**(6):481-489. [doi:10.1016/j.measurement.2005.12.012]
- Kolb, P.W., Decca, R.S., Drew, H.D., 1998. Capacitive sensor for micropositioning in two dimensions. *Rev. Sci. Instrum.*, **69**(1):310-312. [doi:10.1063/1.1148515]
- Kuijpers, A.A., Krijnen, G.J.M., Wiegerink, R.J., Lammerink, T.S.J., Elwenspoek, M., 2006. A micromachined capacitive incremental position sensor. *J. Micromech. Microeng.*, **16**(6):S116-124. [doi:10.1088/0960-1317/16/6/S18]
- Meyer, H.U., 1996. An integrated capacitive position sensor. *IEEE Trans. Instrum. Meas.*, **45**(2):521-525. [doi:10.1109/19.492779]
- Pedrocchi, A., Hoen, S., Ferrigno, G., Pedotti, A., 2000. Perspectives on MEMS in bioengineering: a novel capacitive position microsensor. *IEEE Trans. Biomed. Eng.*, **47**(1):8-11. [doi:10.1109/10.817612]
- Picotto, G.B., Pisani, M., Sosso, A., 2009. A multi-electrode plane capacitive sensor for displacement measurements and attitude controls. *Meas. Sci. Technol.*, **20**(8):1-4. [doi:10.1088/0957-0233/20/8/084011]
- Tolles, W.M., 1996. Nanoscience and nanotechnology in Europe. *Nanotechnology*, **7**(2):59-105. [doi:10.1088/0957-4484/7/2/001]
- Wang, W., Li, X.X., Chen, Z.C., 2008. A planar capacitive sensor for large scale measurement. *Key Eng. Mater.*, **381-382**:509-512. [doi:10.4028/KEM.381-382.509]